

PI(3,5)P₂ controls vacuole potassium transport to support cellular osmoregulation

Zachary N. Wilson, Amber L. Scott, Robin D. Dowell, and Greg Odorizzi*

Department of Molecular, Cellular, and Developmental Biology, University of Colorado, Boulder, CO 80309-0347

ABSTRACT Lysosomes are dynamic organelles with critical roles in cellular physiology. The lysosomal signaling lipid phosphatidylinositol 3,5-bisphosphate (PI(3,5)P₂) is a key regulator that has been implicated to control lysosome ion homeostasis, but the scope of ion transporters targeted by PI(3,5)P₂ and the purpose of this regulation is not well understood. Through an unbiased screen in *Saccharomyces cerevisiae*, we identified loss-of-function mutations in the vacuolar H⁺-ATPase (V-ATPase) and in Vnx1, a vacuolar monovalent cation/proton antiporter, as suppressor mutations that relieve the growth defects and osmotic swelling of vacuoles (lysosomes) in yeast lacking PI(3,5)P₂. We observed that depletion of PI(3,5)P₂ synthesis in yeast causes a robust accumulation of multiple cations, most notably an ~85 mM increase in the cellular concentration of potassium, a critical ion used by cells to regulate osmolarity. The accumulation of potassium and other cations in PI(3,5)P₂-deficient yeast is relieved by mutations that inactivate Vnx1 or inactivate the V-ATPase and by mutations that increase the activity of a vacuolar cation export channel, Yvc1. Collectively, our data demonstrate that PI(3,5)P₂ signaling orchestrates vacuole/lysosome cation transport to aid cellular osmoregulation.

Monitoring Editor

Sandra Lemmon
University of Miami

Received: Jan 5, 2018

Revised: Apr 27, 2018

Accepted: May 17, 2018

INTRODUCTION

Phosphoinositides are a family of regulatory lipids synthesized through the differential phosphorylation of the membrane lipid, phosphatidylinositol. Unique phosphoinositide species are generated on cytosolic membrane surfaces to provide distinct markers that attract effector proteins and regulate the function of resident membrane proteins (Strahl and Thorner, 2007). The control of ion channel and transporter activity is emerging as an important function of phosphoinositide signaling. For example, phosphatidylinositol-4,5-bisphosphate regulates numerous ion channels and transporters at the plasma membrane, including inward-rectifying

K⁺ channels, transient receptor potential channels, and several plasma membrane cation antiporters (Hilgemann and Ball, 1996; Suh and Hille, 2008; Rohacs, 2009). Although phosphoinositides are established as key modulators of plasma membrane ion transport, less is known about phosphoinositide regulation of intracellular ion transport.

A prime candidate regulator of intracellular ion transport is the low-abundant lysosomal phosphoinositide, phosphatidylinositol-3,5-bisphosphate (PI(3,5)P₂). Cellular levels of PI(3,5)P₂ are dynamically regulated by a conserved signaling complex composed of a scaffold protein (Vac14), which localizes to lysosomal membranes and binds the lipid kinase (Fab1 in yeast, PIKfyve in mammals) that phosphorylates the 5'-hydroxyl of phosphatidylinositol-3-phosphate (PI3P) to produce PI(3,5)P₂ (Gary *et al.*, 1998; Sbrissa *et al.*, 1999; Bonangelino *et al.*, 2002; Jin *et al.*, 2008). The Vac14 scaffold also binds a lipid phosphatase (Fig4/Sac3) that removes the 5'-phosphate from PI(3,5)P₂ to yield PI3P (Gary *et al.*, 2002; Sbrissa *et al.*, 2007). This kinase/phosphatase signaling complex can respond to environmental and cellular cues to generate the acute synthesis and turnover of PI(3,5)P₂.

One stimulus that elicits a robust PI(3,5)P₂ signaling event is a high extracellular salt concentration, which causes cellular hyperosmotic stress. Upon hyperosmotic shock, cellular PI(3,5)P₂ levels increase ~20-fold within 15 min and then return to baseline levels, suggesting that PI(3,5)P₂ signaling is involved in the initial adaptive

This article was published online ahead of print in MBoC in Press (<http://www.molbiolcell.org/cgi/doi/10.1091/mbc.E18-01-0015>) on May 23, 2018.

Z.W. and G.O. conceived and designed the experiments, and Z.W. performed the experiments. A.S. performed whole-genome sequencing and analysis under the supervision of R.D. Z.W. wrote the manuscript. G.O. edited the manuscript.

*Address correspondence to: Greg Odorizzi (odorizzi@colorado.edu).

Abbreviations used: Baf-A1, bafilomycin-A1; PI3P, phosphatidylinositol-3-phosphate; PI(3,5)P₂, phosphatidylinositol-3,5-bisphosphate.

© 2018 Wilson *et al.* This article is distributed by The American Society for Cell Biology under license from the author(s). Two months after publication it is available to the public under an Attribution-Noncommercial-Share Alike 3.0 Unported Creative Commons License (<http://creativecommons.org/licenses/by-nc-sa/3.0>).

"ASCB®," "The American Society for Cell Biology®," and "Molecular Biology of the Cell®" are registered trademarks of The American Society for Cell Biology.

response to hyperosmotic stress (Dove *et al.*, 1997; Duex *et al.*, 2006). Cells deficient in PI(3,5)P₂ synthesis are hypersensitive to high extracellular salt concentrations (Jin *et al.*, 2017) and exhibit a dramatic enlargement of endolysosomal organelles that have defects in ion transport (Gary *et al.*, 1998; Ikononov *et al.*, 2001; Nicot *et al.*, 2006; Rusten *et al.*, 2006; Dong *et al.*, 2010; Li *et al.*, 2014). PI(3,5)P₂ signaling, therefore, performs a crucial role in protecting cells against osmotic and ionic stress and may do so by regulating ion transport at endolysosomal organelles.

In mammals, PI(3,5)P₂ is a potent activator of the transient receptor potential mucolipin 1 (TRPML1) channel and of lysosomal two-pore channels, all of which are cation export channels at the lysosomal membrane (Dong *et al.*, 2010; Wang *et al.*, 2012). The yeast orthologue of TRPML1, Yvc1, functions at the lysosome-like vacuole and is activated in response to hyperosmotic stress, and this function of Yvc1 is disabled in the absence of PI(3,5)P₂ synthesis (Denis and Cyert, 2002; Dong *et al.*, 2010). PI(3,5)P₂ has also been proposed to regulate vacuole acidification by adjusting the activity of the vacuolar H⁺-ATPase (V-ATPase) in yeast or by inhibiting an anion/proton exchanger in plants (Li *et al.*, 2014; Ho *et al.*, 2015; Carpaneto *et al.*, 2017). This evidence implies that a conserved role of PI(3,5)P₂ signaling is to control the transport of ions or other metabolites at the vacuole/lysosome. However, the cohort of transporters regulated by PI(3,5)P₂ is not well defined, and it is unclear how the regulation of vacuole/lysosome ion transport by PI(3,5)P₂ signaling is tied to specific lysosomal or cellular processes.

In this study, we identify loss-of-function mutations in vacuolar cation transporters as mutations that suppress the growth defect and the vacuolar and cellular enlargement phenotypes of *fab1Δ* yeast cells, which completely lack PI(3,5)P₂ synthesis. We demonstrate that *fab1Δ* cells accumulate several cations, most notably a robust increase in cellular potassium, which is the most abundant cation in cells and a critical cellular osmolyte. Collectively, our data suggest a model for how PI(3,5)P₂ signaling regulates vacuolar potassium transport to protect cells against osmotic stress.

RESULTS

Identification of mutations that bypass the loss of PI(3,5)P₂

Saccharomyces cerevisiae is one of the few model organisms known to survive without PI(3,5)P₂, which can be produced in yeast only through the activity of the PI3P-5-kinase, Fab1. Yeast lacking the *FAB1* gene (*fab1Δ*) replicate slowly, spontaneously lyse, and are sensitive to many stressors, including high temperature (Yamamoto *et al.*, 1995). These phenotypes occasionally revert, as *fab1Δ* yeast frequently produce spontaneous suppressor mutations when grown at the nonpermissive temperature of 37°C. Because genetic suppressor mutations often identify genes functioning within similar pathways, we decided to analyze suppressor mutants of *fab1Δ* yeast. Sixteen clonal, haploid *fab1Δ* strains with spontaneous suppressor mutations that enable growth at 37°C were cataloged as *fab1Δbfo1–16* for Bypass Fab1. Backcrossing each *fab1Δbfo* suppressor strain with a *fab1Δ* strain of the opposite mating type produced diploid strains unable to grow at 37°C, indicating that each *bfo* mutation was recessive (unpublished data). Crossing the *fab1Δbfo* strains with one another and testing the growth of resulting diploids at 37°C revealed that the 16 *bfo* mutations belonged to two complementation groups. Whole-genome sequencing of one representative strain from each *bfo* complementation group (*fab1Δbfo3* and *fab1Δbfo14*) identified unique mutations in two genes, *VPH1* and *VNX1*, both of which are involved in vacuole ion transport (Figure 1A).

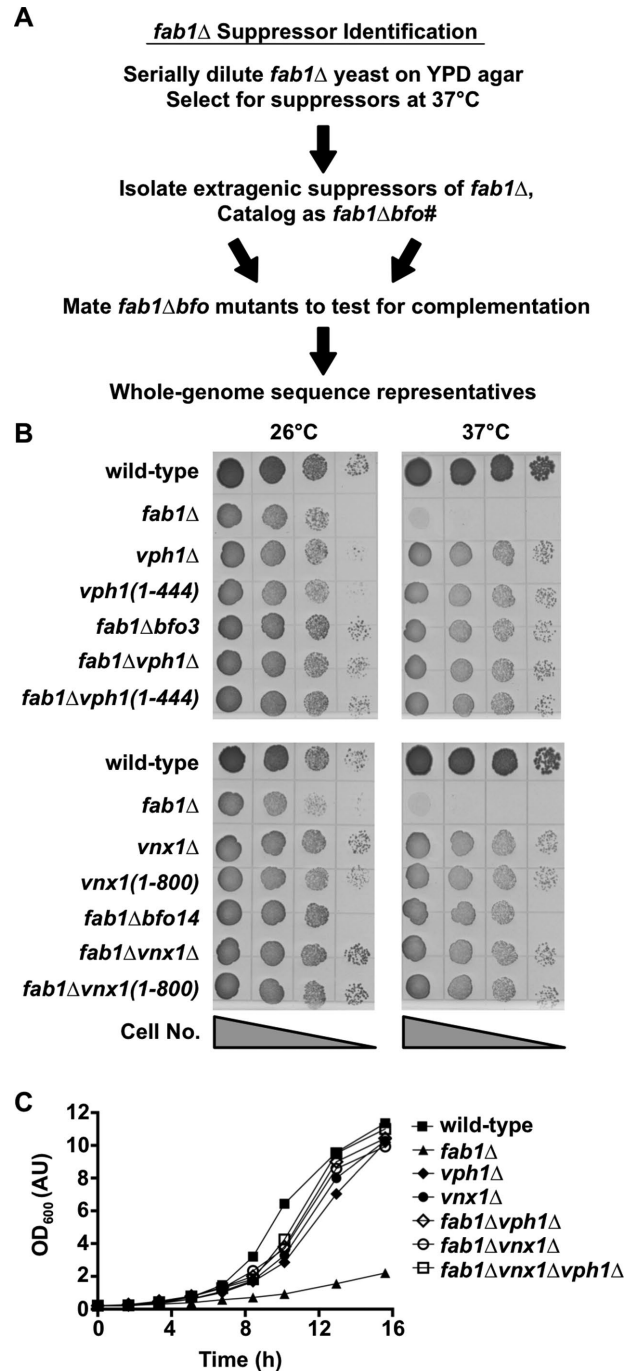


FIGURE 1: Identification of mutations that bypass the loss of Fab1. (A) Flowchart of the methodology used to isolate and identify suppressor mutations of *fab1Δ* yeast. Suppressor strains were denoted *fab1Δbfo(1-16)*, which stands for Bypass Fab1. (B) Cell growth assay of the indicated yeast strains on rich agar medium at 26°C or 37°C for 3 d. Shown is a representative assay of three independent experiments. (C) Growth curves of the indicated yeast strains in rich liquid medium at 26°C. Shown is a representative growth curve of three independent experiments.

VPH1 encodes subunit “a” of the membrane-embedded domain of the V-ATPase, and *VNX1* encodes a monovalent cation/proton antiporter at the vacuole membrane (Kane, 2006; Cagnac *et al.*, 2007). Sanger sequencing of the *VPH1* and *VNX1* loci in the other 14 *fab1Δbfo* suppressor strains indicated the presence of

Strain	VPH1 mutation	VNX1 mutation
<i>fab1Δbfo1</i>	Frameshift (nt 1334–1353 deleted)	–
<i>fab1Δbfo2</i>	Nonsense (E404*)	–
<i>fab1Δbfo3[†]</i>	Frameshift (nt 1334–1353 deleted)	–
<i>fab1Δbfo4</i>	Nonsense (E404*)	–
<i>fab1Δbfo5</i>	Nonsense (E404*)	–
<i>fab1Δbfo6</i>	Nonsense (E404*)	–
<i>fab1Δbfo7</i>	Frameshift (E404*)	–
<i>fab1Δbfo8</i>	Frameshift (nt 715–716 deleted)	–
<i>fab1Δbfo9</i>	–	Nonsense (S801*)
<i>fab1Δbfo10</i>	Nonsense (E404*)	–
<i>fab1Δbfo11</i>	–	Nonsense (Q620*)
<i>fab1Δbfo12</i>	–	Frameshift (nt 1760 deleted)
<i>fab1Δbfo13</i>	–	Nonsense (Q459*)
<i>fab1Δbfo14[†]</i>	–	Nonsense (S801*)
<i>fab1Δbfo15</i>	–	Nonsense (Q459*)
<i>fab1Δbfo16</i>	Nonsense (Y328*)	–

nt, nucleotide of coding sequence; *, stop codon.

TABLE 1: Mutations in *fab1Δbfo* suppressor strains identified by whole-genome sequencing (†) or by Sanger sequencing of the *VPH1* or *VNX1* locus.

mutations predicted to disrupt the function of either the *VPH1* or *VNX1* gene product (Table 1). To confirm that suppression of *fab1Δ* growth defects stem from the loss of Vph1 or Vnx1 protein function, we deleted the *VPH1* or *VNX1* gene in a naive *fab1Δ* strain, resulting in *fab1Δvph1Δ* and *fab1Δvnx1Δ*; in parallel, we introduced into a naive *fab1Δ* strain the truncating mutations that were identified by whole-genome sequencing of the *fab1Δbfo3* and *fab1Δbfo14* strains, creating *fab1Δvph1(1–444)* and *fab1Δvnx1(1–800)*. Both deletion and truncation of either Vph1 or Vnx1 suppressed the temperature-sensitive growth of *fab1Δ* yeast (Figure 1B). Additionally, adding back the wild-type *VPH1* or *VNX1* gene encoded on a low-copy plasmid restored temperature-sensitive growth at 37°C to the *fab1Δbfo3* and *fab1Δbfo14* suppressor strains, respectively (Supplemental Figure S1A). Importantly, the *fab1Δvph1Δ* and *fab1Δvnx1Δ* double-mutant strains and a *fab1Δvph1Δvnx1Δ* triple-mutant strain each demonstrated a significant enhancement in growth at the permissive temperature of 26°C compared with the *fab1Δ* parent strain (Figure 1C). Deletion of *VPH1* and/or *VNX1* also suppressed the salt sensitivity of *fab1Δ* yeast (Supplemental Figure S1B). Therefore, disruption of Vph1 or Vnx1 function generally suppresses the growth defect of *fab1Δ* cells.

To determine whether the loss of either Vph1 or Vnx1 bypasses a deficiency specifically in PI(3,5)P₂ signaling, we deleted *VPH1* or *VNX1* in yeast lacking either Vac7 or Vac14, each of which is required for activation of Fab1 kinase function (Bonangelino *et al.*, 2002; Gary *et al.*, 2002). Like *fab1Δ* cells, the *vac7Δ* and *vac14Δ* mutant strains exhibit temperature-sensitive growth, which was suppressed by deleting *VPH1* or *VNX1* (Supplemental Figure S1C). Suppression was also observed upon disrupting Vph1 or Vnx1 function in yeast expressing either the temperature-sensitive *fab1^{ts}* allele, which lacks PI3P 5-kinase activity at 37°C, or the *fab1^{D2314R}* allele, which has a point mutation in the kinase domain that abolishes PI(3,5)P₂ synthesis (Gary *et al.*, 1998; Supplemental Figure S1, C and D). In contrast, deleting the *VPH1* or *VNX1* gene did not suppress temperature-sensitive growth of *vps34Δ* yeast, which lack the

Vps34 PI 3-kinase that functions upstream of Fab1 by synthesizing PI3P (Supplemental Figure S1C). Therefore, loss-of-function mutations in either Vph1 or Vnx1 suppress the growth defects of yeast that are specifically deficient in PI(3,5)P₂ signaling.

Inhibiting vacuole acidification suppresses temperature-sensitive growth of *fab1Δ* yeast

The V-ATPase is a multisubunit proton pump that hydrolyzes ATP to transport protons into the Golgi, endosomes, and lysosomes/vacuoles (Kane, 2006). In *S. cerevisiae*, each subunit of the V-ATPase is encoded by a single gene, with one exception: the Vph1 subunit is specific to V-ATPase complexes that are targeted to the vacuole membrane. V-ATPases that function at the Golgi/endosomes lack Vph1 and, instead, have Stv1, which is structurally and functionally similar to Vph1 but contains a Golgi/endosomal retention signal (Finnigan *et al.*, 2012). Unlike the *VPH1* deletion, deleting *STV1* failed to suppress the temperature-sensitive growth of *fab1Δ* yeast (unpublished data). General disruption of the V-ATPase by deletion of its other subunit genes in *fab1Δ* cells also did not suppress temperature-sensitive growth but, instead, caused synthetic lethality, presumably because the loss of both the Golgi/endosomal and the vacuolar V-ATPase functions cannot be tolerated in the absence of Fab1 activity (Supplemental Figure S2A).

Discovering inactivating mutations in the vacuolar/Vph1-specific V-ATPase that suppress the growth defects of *fab1Δ* yeast prompted us to examine whether loss of vacuole acidification is the mechanism by which suppression occurs. To assess vacuole acidification within *fab1Δ* and *fab1Δvph1Δ* cells, we chromosomally integrated superecliptic pHluorin in frame with the C-terminus of Sna3 (Sna3-pHluorin). Sna3 is a protein that is directed to the vacuole lumen, as demonstrated by the vacuolar localization of a Sna3-GFP fusion (Figure 2A). Unlike GFP, the fluorescence of Sna3-pHluorin is quenched at pH values below ~6; thus, very little fluorescence signal from Sna3-pHluorin is detected in wild-type yeast vacuoles, which have been reported to contain a pH of ~5.5 (Sankaranarayanan *et al.*, 2000;

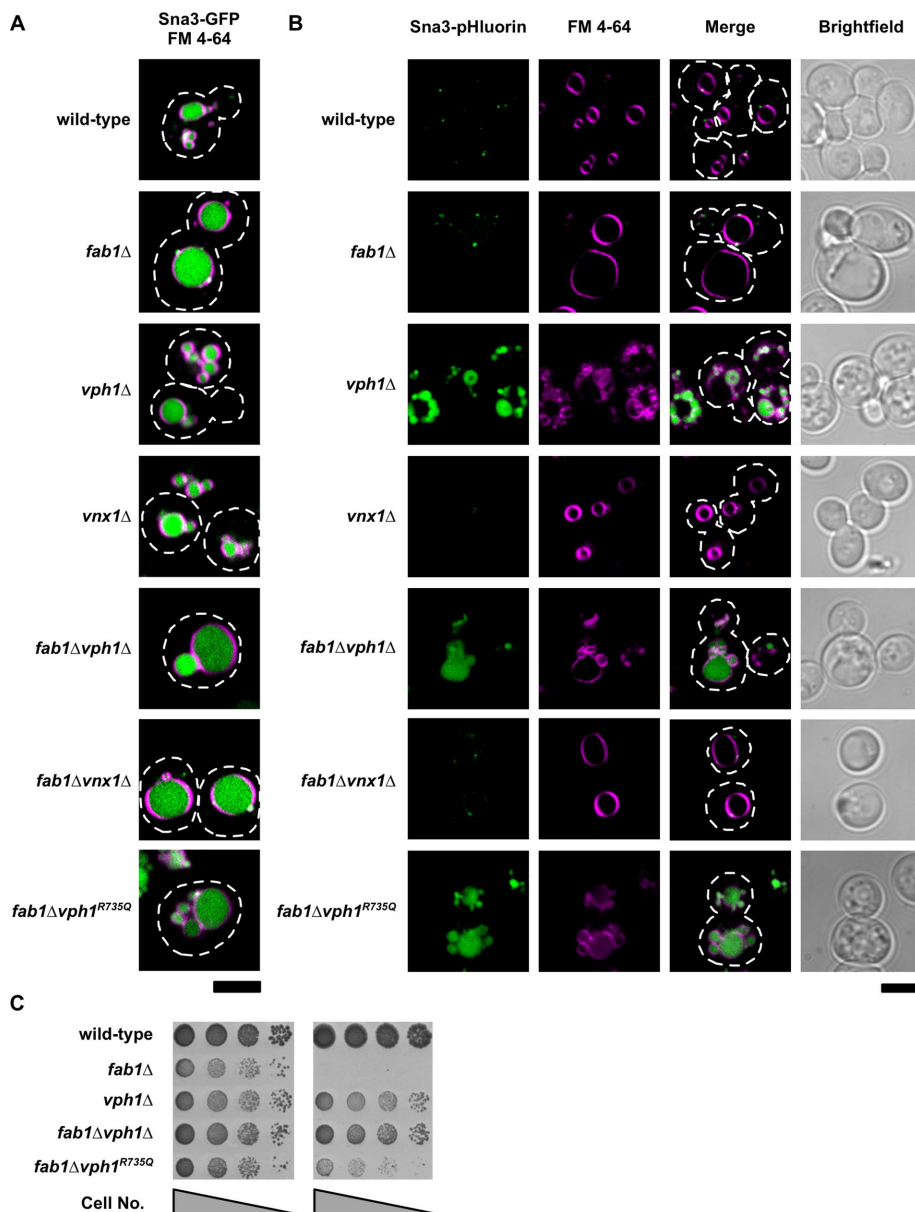


FIGURE 2: Inhibiting vacuole acidification suppresses temperature-sensitive growth of *fab1Δ* yeast. Live-cell confocal fluorescence microscopy analysis of Sna3-GFP (A) and Sna3-pHluorin (B) in the indicated yeast strains. The vacuole membrane is stained with the lipophilic fluorescent dye, FM 4-64. Dashed lines represent cell outlines. Scale bar = 4 μ m. (C) Cell growth assay of the indicated yeast strains grown on rich agar medium plates at 26°C or 37°C for 3 d. Shown is a representative assay of three independent experiments.

Prosser *et al.*, 2010). In contrast, Sna3-pHluorin fluorescence is observed in the vacuoles of *vph1Δ* and *fab1Δvph1Δ* cells, as expected, because these strains no longer contain vacuolar (Vph1-specific) V-ATPases (Figure 2B). In support of recent evidence that *fab1Δ* vacuoles are acidified (Ho *et al.*, 2015), we did not detect Sna3-pHluorin fluorescence in the vacuole lumen of *fab1Δ* cells (Figure 2B). Thus, yeast lacking PI(3,5)P₂ have acidified vacuoles, and vacuole acidification is lost upon disruption of Vph1 function.

To disable vacuole acidification yet maintain the structural integrity of the vacuolar V-ATPase complex, we replaced the wild-type *VPH1* gene with the *vph1^{R735Q}* mutant allele, which encodes a Vph1 protein product with a point mutation that disrupts proton pumping without affecting the assembly or trafficking of the V-ATPase

(Kawasaki-Nishi *et al.*, 2001; Coonrod *et al.*, 2013). Expression of Sna3-pHluorin in the *fab1Δvph1^{R735Q}* strain confirmed that the vacuoles are no longer acidic (Figure 2B). The *fab1Δvph1^{R735Q}* mutant strain grows at 37°C (Figure 2C), consistent with a loss in vacuole acidification being responsible for suppression of the temperature-sensitive growth defect in *fab1Δ* cells. However, *fab1Δvph1^{R735Q}* cells did not grow as well as *fab1Δvph1Δ* cells (Figure 2C), potentially signifying that *vph1^{R735Q}* acts as a dominant-negative mutation that competes with Stv1 in the assembly of functional V-ATPase complexes.

Overexpression of Stv1, the Vph1 paralogue specific to Golgi/endosomal V-ATPase complexes, has been shown to suppress some phenotypes associated with the loss of Vph1 function because excess Stv1-containing V-ATPases saturate the Golgi/endosomal retention machinery and are consequently trafficked to the vacuole (Finnigan *et al.*, 2012; Sardon *et al.*, 2014). Indeed, overexpression of the *STV1* gene from a high-copy (2 μ) plasmid restores temperature-sensitive growth to *fab1Δvph1Δ* cells and recovers vacuole acidification but does not affect the growth phenotypes of wild-type or *fab1Δ* yeast (Supplemental Figure S, B and C). Temperature-sensitive growth is also restored to *fab1Δvph1Δ* cells upon heterologous expression of the *Arabidopsis thaliana* vacuolar H⁺-translocating inorganic pyrophosphatase, Avp1, which can independently acidify yeast vacuoles at the expense of pyrophosphate (Coonrod *et al.*, 2013; Supplemental Figure S2D). Together, these results establish that inhibiting vacuole acidification enhances the growth of yeast lacking PI(3,5)P₂ synthesis by Fab1.

The *vph1* and *vnx1* suppressor mutations reduce vacuole size in PI(3,5)P₂-deficient yeast

PI(3,5)P₂ signaling is an important regulator of vacuole/lysosome morphology, and a consequence of PI(3,5)P₂ depletion is dramatic swelling of endolysosomal organelles. Because the V-ATPase and ion transporters like Vnx1 have been shown to regulate homotypic vacuole fusion events, we investigated whether the inhibition of Vph1 or Vnx1 function suppresses vacuole enlargement in *fab1Δ* yeast by blocking vacuole fusion to cause vacuole fragmentation (Baars *et al.*, 2007; Qiu and Fratti, 2010). In *S. cerevisiae*, vacuole morphology provides an index of the *in vivo* equilibrium between vacuole fusion and fission. Using the lipophilic fluorescent dye FM 4-64 to visualize yeast vacuoles, wild-type yeast typically contain 1–3 vacuoles per cell (Figure 3, A and B). On the two opposite extremes, *fab1Δ* yeast contain single, enlarged vacuoles (in 85% of cells; Figure 3B), in part, due to defects in vacuole fission (Dove *et al.*, 2004; Zieger and Mayer, 2012), whereas *vph1Δ* cells have fragmented

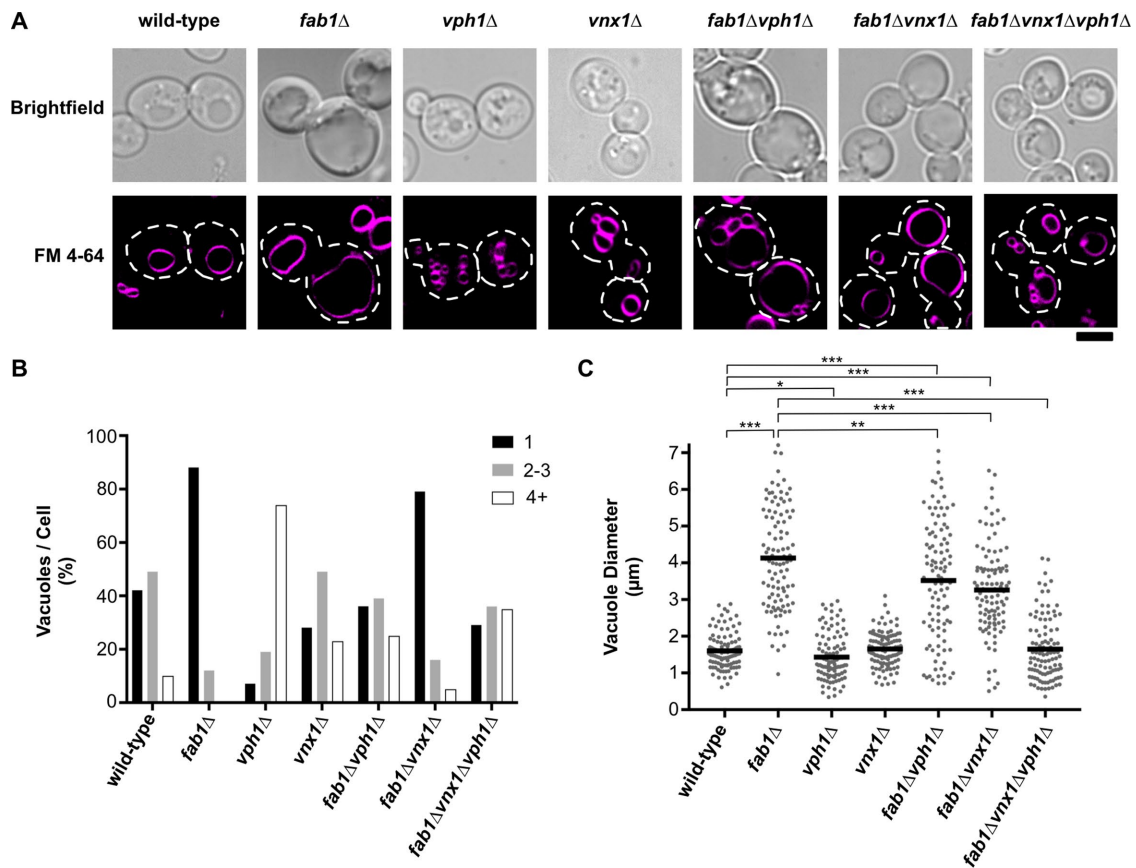


FIGURE 3: Vacuole morphology of *fab1Δ* yeast and bypass suppressor strains. (A) Live-cell confocal fluorescence microscopy analysis of the vacuole morphology of the indicated yeast strains. Vacuoles were visualized with FM 4-64, representative images of which are shown with corresponding brightfield images. Dashed lines represent cell outlines. Scale bar = 4 μm. (B) Quantitation of the number of vacuoles observed per cell of the strains imaged in A by counting FM 4-64-labeled organelles ($n > 100$ cells per strain). (C) Quantitation of vacuole diameter measurements taken by a line-scan analysis of FM 4-64-labeled vacuoles. Diameters were measured for only the largest vacuole observed per cell for the strains indicated. Each dot represents a single vacuole, with the horizontal line representing the mean of all measurements ($n = 104$ per strain). Unpaired *t* tests with Welch's correction were used to determine statistical significance; **, $P < 0.01$ and ***, $P < 0.001$. Unless otherwise indicated, all other mutant strains were not statistically different compared with the wild-type control.

vacuoles (74% of cells display ≥ 4 vacuoles/cell; Figure 3B) caused by dysfunctions in vacuole fusion (Baars *et al.*, 2007). Interestingly, although we did observe a modest increase in vacuole fragmentation in *fab1Δvph1Δ* (24% of cells display ≥ 4 vacuoles/cell), there was still a significant population of cells with single, enlarged vacuoles (40% of cells; Figure 3B). Similarly, although the *vnx1Δ* single-mutant strain showed a modest increase in vacuole fragmentation (23% of cells display ≥ 4 vacuoles/cell), the *fab1Δvnx1Δ* suppressor strain had a vacuole morphology almost identical to that of *fab1Δ* yeast (77% of cells contain single, enlarged vacuoles; Figure 3, A and B). These observations suggested that blocking vacuole fusion in *fab1Δ* cells is not sufficient to suppress the growth defect caused by the loss of PI(3,5)P₂ signaling. Indeed, removing genes that directly participate in vacuole homotypic fusion (*MON1* [a GEF for the Rab, Ypt7], *VPS41* [a subunit of the HOPS membrane tethering complex], or *VAM3* [a vacuolar Q-SNARE]) failed to rescue the growth of *fab1Δ* yeast at 37°C (Supplemental Figure S3, A and B).

In our survey of the vacuole morphology of *fab1Δ* and *fab1Δvnx1Δ* yeast, we noticed that the single, enlarged vacuoles of *fab1Δvnx1Δ* cells appeared reduced in size compared with those found in *fab1Δ* cells. To compare vacuole size between strains, we measured the

diameter of the largest vacuole observed per cell for >100 cells per strain. Notably, the mean vacuole diameter observed in *fab1Δvnx1Δ* cells is reduced by ~25% (mean vacuole diameter of 3.2 μm; Figure 3C) compared with *fab1Δ* cells (mean vacuole diameter of 4.1 μm; Figure 3C), which is equivalent to almost halving the total vacuole volume. In support of the idea that the *vph1Δ* and *vnx1Δ* mutations reduce vacuole size in *fab1Δ* cells, a *fab1Δvph1Δvnx1Δ* triple-mutant strain showed complete suppression of the vacuole enlargement phenotype of *fab1Δ* yeast (Figure 3, A–C), with a vacuole morphology very similar to wild type and rarely ($<8\%$ of cells) containing vacuoles exceeding 3 μm in diameter (Figure 3C). These data suggest that blocking both vacuole acidification and Vnx1 function act synergistically to reduce the enlarged vacuole phenotype of yeast deficient in PI(3,5)P₂ signaling.

Acute inhibition of V-ATPase function blocks vacuole enlargement upon loss of PI(3,5)P₂ synthesis

To determine whether the vacuole proton gradient is required for vacuoles to enlarge upon depletion of PI(3,5)P₂ synthesis, we acutely blocked V-ATPase function in *fab1^{ts}* cells with a V-ATPase inhibitor, bafilomycin-A1 (Baf-A1). The *fab1^{ts}* strain expresses a mutant Fab1

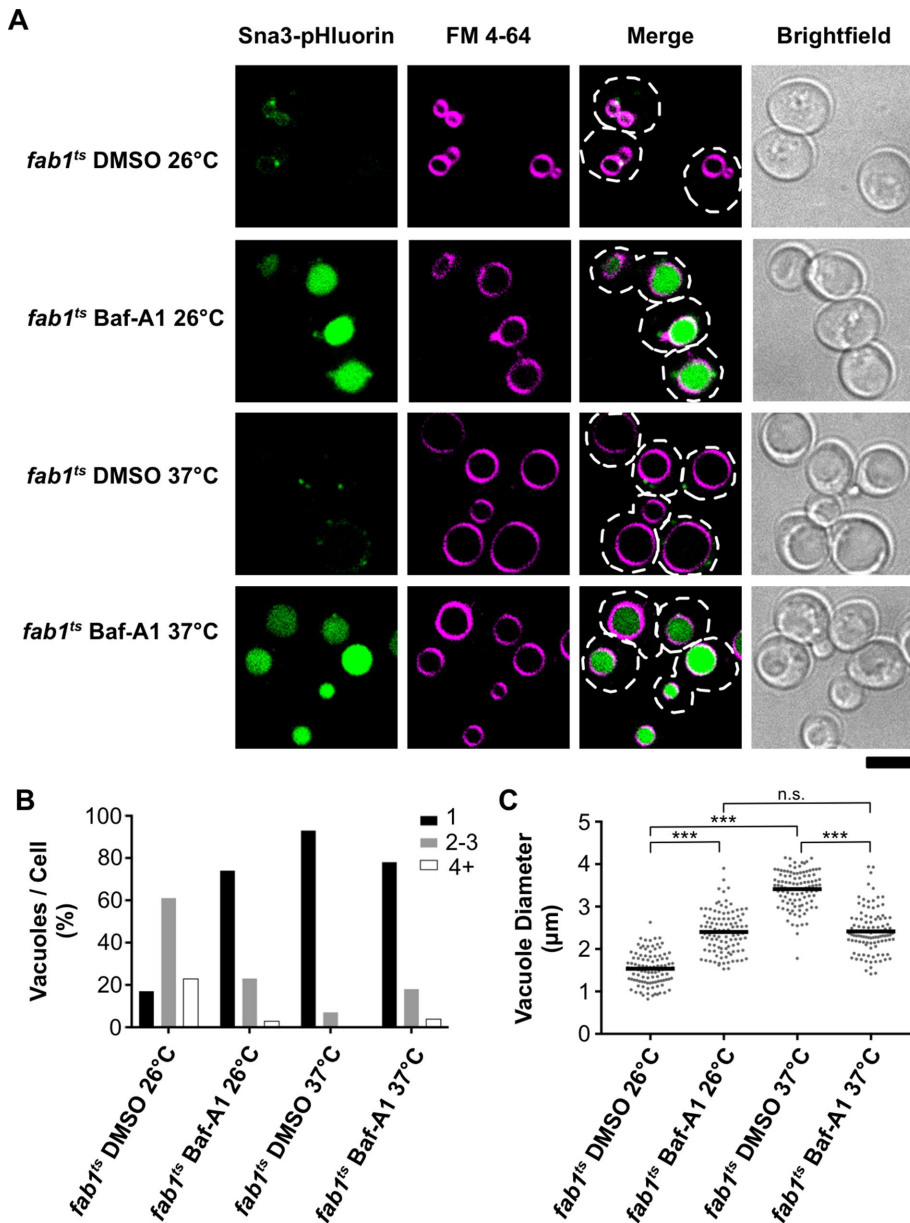


FIGURE 4: Acute inhibition of vacuole acidification blocks vacuole enlargement in *fab1^{ts}* cells. (A) Live-cell confocal fluorescence microscopy analysis of the vacuole morphology and Sna3-pHluorin fluorescence in *fab1^{ts}* cells. Images were taken after a 2-h incubation at the indicated temperature and treated with either vehicle (DMSO) or 10 μ M bafilomycin-A1 (Baf-A1). The vacuole membrane is stained with FM 4-64. Dashed lines represent cell outlines. Scale bar = 4 μ m. (B) Quantitation of the number of vacuoles observed per cell in *fab1^{ts}* for the conditions imaged in A by counting FM 4-64-labeled organelles ($n > 100$ cells per strain). (C) Quantitation of vacuole diameter measurements taken by a line-scan analysis of FM 4-64-labeled vacuoles. Diameters were measured for only the largest vacuole observed per cell. Each dot represents a single vacuole, with the horizontal line representing the mean of all measurements ($n = 104$ per strain). Unpaired *t* tests with Welch's correction were used to determine statistical significance; n.s., not significant; ***, $P < 0.001$.

kinase that cannot synthesize PI(3,5)P₂ at the restrictive temperature of 37°C; consequently, PI(3,5)P₂ levels become undetectable in *fab1^{ts}* cells shortly after a shift to 37°C (Gary et al., 1998). Thus, the *fab1^{ts}* strain can be used to visualize alterations in vacuole morphology that occur after PI(3,5)P₂ depletion. At the permissive temperature (26°C), *fab1^{ts}* cells present a vacuole morphology very similar to wild-type yeast (Figure 4, A–C). In contrast, *fab1^{ts}* cells shifted to

37°C for 2 h present a vacuole morphology similar to *fab1 Δ* yeast (Figure 4A), with most cells containing single, enlarged vacuoles (93% of cells; Figure 4B) having a mean vacuole diameter of \sim 3.5 μ m (Figure 4C). Notably, vacuole enlargement was inhibited by the addition of 10 μ M Baf-A1 to *fab1^{ts}* cells at the start of their 2-h incubation at 37°C, as the vacuoles expanded to a mean vacuole diameter of only \sim 2.4 μ m (Figure 4, A and C). The moderate expansion of vacuole diameter in *fab1^{ts}* cells treated with Baf-A1 appears to be an effect of V-ATPase inhibition, as vacuoles became slightly enlarged upon Baf-A1 treatment, no matter if the cells were incubated at 26°C or 37°C (Figure 4, A and C). Indeed, we observed a similar effect in wild-type yeast treated with Baf-A1 (Supplemental Figure 4, A and C), and this vacuole morphology is consistent with the vacuole morphology observed in *vma* mutants that lack the nonredundant subunits of the V-ATPase (Baars et al., 2007).

Importantly, we used Sna3-pHluorin to demonstrate that Baf-A1 was inhibiting vacuole acidification in *fab1^{ts}* and wild-type yeast (Figure 4A and Supplemental Figure 4A). Similar to our observation in *fab1 Δ* cells, we could not detect Sna3-pHluorin fluorescence in *fab1^{ts}* cells shifted to 37°C in the absence of Baf-A1, further confirming that cells lacking PI(3,5)P₂ synthesis still contain acidified vacuoles (Figure 4A). Taken together, our results demonstrate that the vacuole proton gradient is required for the dramatic vacuole expansion phenotype observed in cells defective for PI(3,5)P₂ synthesis.

Cation content is increased in *fab1 Δ* yeast cells

An emerging function for PI(3,5)P₂ signaling is the regulation of ion transport across the lysosome/vacuole membrane. One hypothesis for the enlarged vacuole phenotype of *fab1 Δ* yeast is that the vacuoles aberrantly accumulate specific osmolytes that cause osmotic swelling of the vacuole. Potassium ions are the primary osmolyte utilized by yeast to maintain cell turgor and to balance the negative charge of essential organic anions (Arino et al., 2010). Considering Vnx1 is the primary transporter of potassium into the yeast vacuole (Cagnac et al., 2007; Herrera et al., 2013), we hypothesized that both the

vph1 and *vnx1* suppressor mutations inhibit the import of this important osmolyte into the vacuole, either by directly removing Vnx1 or by abolishing the proton gradient used by Vnx1 to power the import of cations. In support of this hypothesis, both *vnx1 Δ* and *fab1 Δ vnx1 Δ* yeast have acidified vacuoles (Figure 2B), indicating that a loss of vacuole acidification is not the means by which Vnx1 disruption suppresses mutant phenotypes in *fab1 Δ* cells.

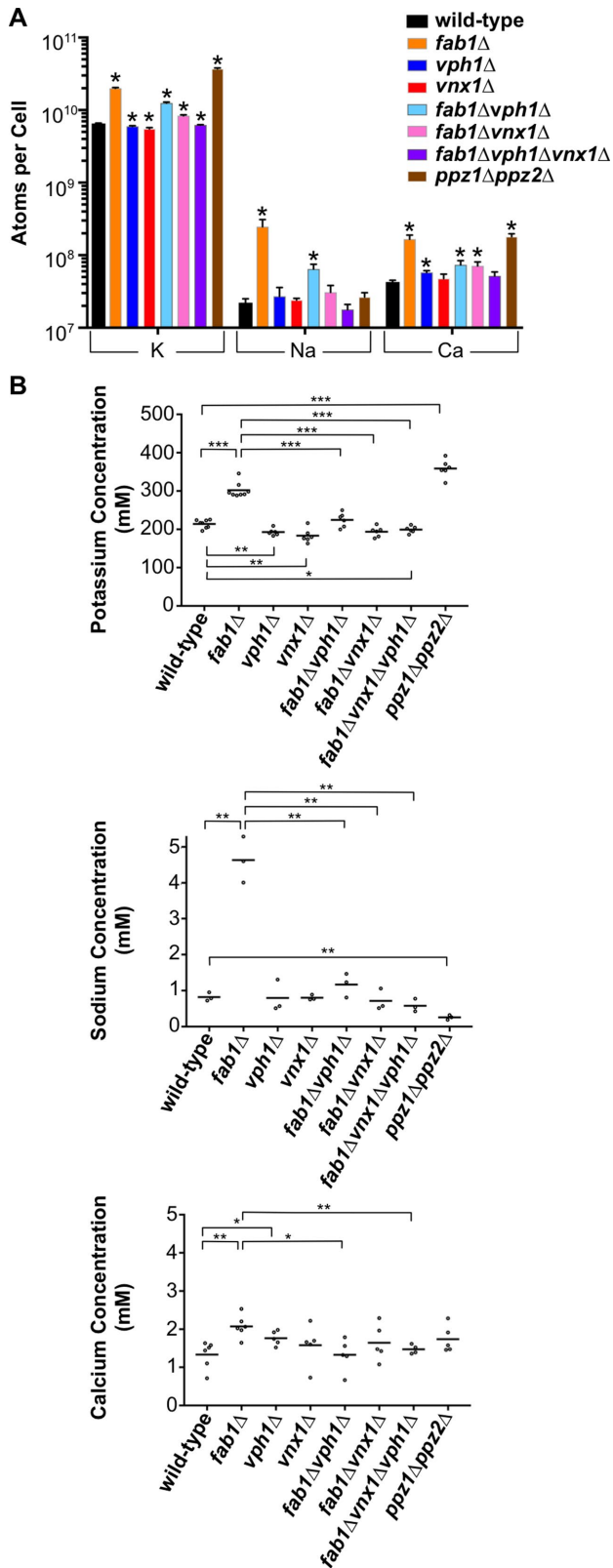


FIGURE 5: Cation content is increased in *fab1Δ* yeast. (A) Quantitation of the total K, Na, and Ca molecules observed per cell for each of the strains indicated, as determined by ICP-AES. The bars represent the mean, error bars show the SD of three or more independent experiments and unpaired t tests with Welch's correction were used to determine statistical significance; *, $P < 0.05$. Unless otherwise indicated, all other mutant strains were not

We directly determined the cellular content of potassium in *fab1Δ* cells using inductively coupled plasma atomic emission spectroscopy (ICP-AES). Strikingly, *fab1Δ* yeast contained an approximately threefold increase in total potassium levels compared with the wild-type parent strain (Figure 5A and Supplemental Figure S5A). An increase in ion content would generally be expected due to the twofold larger size of *fab1Δ* cells compared with wild-type cells (~110 μm^3 compared with ~50 μm^3 ; Figure 6B). However, even after taking into account the difference in their volumes, *fab1Δ* cells contain an ~85 mM increase in total potassium concentration (~300 mM) compared with the potassium concentration in wild-type cells (~215 mM; Figure 5B).

We also investigated the total levels of sodium, calcium, magnesium, and phosphorous, all of which are common elements stored at higher concentrations in yeast vacuoles (Beeler *et al.*, 1997; Li and Kane, 2009; Herrera *et al.*, 2013). Importantly, the values we determined for all of these elements in our wild-type strain (SEY6210) are nearly identical to their concentrations previously reported in different wild-type yeast strains (Eide *et al.*, 2005; van Eunen *et al.*, 2010). Similar to the observed increase in potassium content, *fab1Δ* cells also contained elevated sodium and calcium levels, but the molar increase in each of these ions (~3.8 and ~0.7 mM, respectively) was far less than the ~85 mM increase in potassium in *fab1Δ* cells relative to wild-type yeast (Figure 5, A and B). Conversely, we observed a decrease in phosphorous content (~180 mM in *fab1Δ* yeast compared with ~250 mM in wild-type yeast), matched with a concomitant decrease in total magnesium levels (~18 mM in *fab1Δ* yeast compared with ~35 mM in wild-type yeast; Supplemental Figure S5, A and B). We also observed an ~2.1-fold increase in total sulfur content that results in equivalent sulfur concentrations in both wild-type and *fab1Δ* yeast, demonstrating that the loss of PI(3,5)P₂ signaling does not, in general, affect the concentrations of all biologically relevant elements (Supplemental Figure S5, A and B).

The increase in potassium, sodium, and calcium ion content observed in *fab1Δ* cells was strongly reverted in *fab1Δvph1Δ*, *fab1Δvnx1Δ*, and *fab1Δvph1Δvnx1Δ* cells (Figure 5, A and B). Overall, the ion composition of each *fab1Δ* suppressor strain mirrored the ionic profiles for the corresponding *vph1Δ* or *vnx1Δ* single-mutant strains. All of the mutants contained similar total concentrations of potassium, sodium, and calcium compared with wild-type yeast, with only modest differences observed in some cases (Figure 5, A and B). Of note, both *vph1Δ* and *vnx1Δ* single mutants demonstrated a significant decrease in total potassium levels, confirming that these transporters are required to maintain the cellular levels of potassium (Figure 5B; Herrera *et al.*, 2013). Every strain lacking VPH1 showed a strong reduction in total phosphorous and magnesium levels (~60–70% the concentration of wild-type yeast; Supplemental Figure S5, A and B), supporting previous reports that the vacuolar proton gradient is required for the proper storage of polyphosphate, which complexes with magnesium in the vacuole (Beeler *et al.*, 1997; Castrol *et al.*, 1999). Even *vnx1Δ* yeast showed

statistically different compared with the wild-type control. Supplemental Figure 5A provides the same values on a linear scale. (B) Concentrations for each of the elements analyzed in A for the yeast strains indicated. Each dot represents the mean of a single analysis with two technical replicates, while the horizontal line denotes the mean of three or more independent experimental replicates. Unpaired t tests with Welch's correction were used to determine statistical significance; *, $P < 0.05$; **, $P < 0.01$; and ***, $P < 0.001$. Unless otherwise indicated, all other mutant strains were not statistically different compared with the wild-type control.

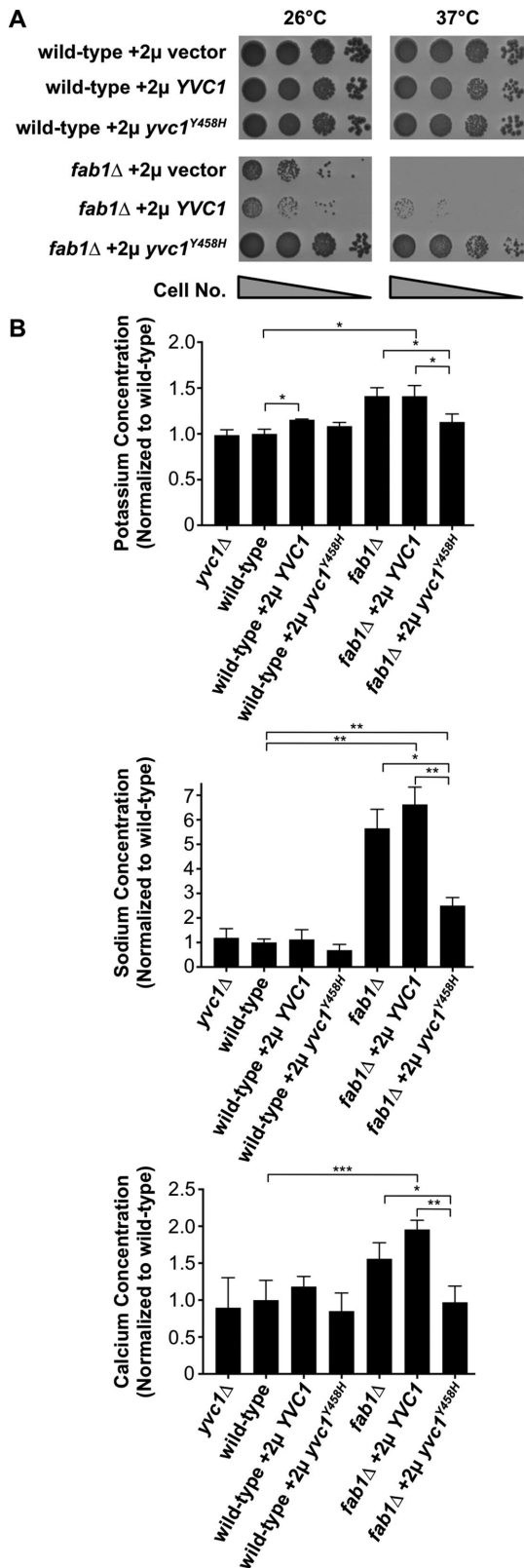


FIGURE 6: Yvc1 gain of function suppresses the temperature sensitivity and cation accumulation of *fab1* Δ yeast. (A) Cell growth assays of the indicated yeast strains grown on minimal agar medium at 26°C or 37°C for 4 d. All strains were transformed with a high-copy number plasmid (2 μ) that was either empty (pRS424) or contained YVC1 or yvc1^{Y458H}. (B) Whole-cell concentrations for K, Na, and Ca observed in the yeast strains indicated by ICP-AES and represented as a ratio compared with wild-type yeast. Bars represent the mean,

a substantial reduction in phosphorous levels (~80% that of wild-type levels), suggesting that monovalent cation import is required to balance the negative charge generated by polyphosphate storage (Supplemental Figure S5, A and B). These data demonstrate that both VPH1 and VNX1 are epistatic to FAB1 with respect to their impact on cellular ion levels, most likely due to their effect on storage of these elements within the vacuole.

Expression of a gain-of-function vacuolar cation export channel bypasses PI(3,5)P₂ deficiency

Considering PI(3,5)P₂ is an activating ligand for the vacuole-localized, cation-conductance channel, Yvc1, we hypothesized that Yvc1 inactivation in *fab1* Δ cells might contribute to the cation accumulation phenotype we observe in *fab1* Δ cells. This idea is supported by the observation that overexpression of the Yvc1 orthologue, TRPML1, caused a decrease in the dramatic lysosome enlargement phenotype of mammalian cells that have reduced PI(3,5)P₂ levels (Dong et al., 2010). However, a similar effect has not been observed in yeast. In fact, we found that overexpressing wild-type YVC1 from a high-copy 2 μ plasmid was incapable of suppressing the temperature sensitivity, cation accumulation, and vacuole enlargement phenotypes of *fab1* Δ yeast (Figure 6, A and B; Supplemental Figure S6, A and C).

Because PI(3,5)P₂ has been shown to be essential for Yvc1 function (Dong et al., 2010), we examined whether a Yvc1 gain-of-function mutation is capable of suppressing the mutant phenotypes of *fab1* Δ yeast. Mutating Y458H in the sixth transmembrane helix destabilizes the gating of Yvc1, creating a Yvc1 gain-of-function mutant protein that has an increase in the open-state probability and an increase in cation discharges from the vacuole lumen (Zhou et al., 2007). Overexpressing the Yvc1^{Y458H} protein in *fab1* Δ yeast recovered growth at 37°C and caused a ~25% decrease in the mean diameter of the largest vacuole observed per cell, mirroring the results observed in the *fab1* Δ vnx1 Δ suppressor strain (Figure 6A; Supplemental Figure S6, A and C). Furthermore, ion content analysis revealed that overexpression of the gain-of-function Yvc1^{Y458H} mutant protein was capable of restoring the cation levels of *fab1* Δ cells to near wild-type concentrations (Figure 6B). Importantly, a yvc1 Δ strain contained levels of potassium, sodium, and calcium that were equivalent to wild-type yeast (Figure 6B), and yvc1 Δ cells presented a normal vacuole morphology (Supplemental Figure S6, A–C), indicating that the loss of Yvc1 activation by PI(3,5)P₂ is not sufficient, on its own, to drive the accumulation of cations or cause the extreme vacuole swelling observed in *fab1* Δ cells.

Our discovery that inactivating mutations in either Vnx1 or the V-ATPase and an activating mutation in Yvc1 all act as suppressor mutations of *fab1* Δ yeast implies that hyperactive cation import into vacuoles occurs in response to the loss of PI(3,5)P₂. Therefore, we sought to determine whether inhibiting other vacuole cation importers could also recover the mutant phenotypes of *fab1* Δ yeast. The growth of *fab1* Δ yeast at 37°C was not rescued by genetic deletion of VCX1 (Ca²⁺/H⁺ antiporter) or PMC1 (Ca²⁺ ATPase), both of which encode transporters that import calcium into the vacuole lumen (Supplemental Figure S7A). Similarly, deletion of NHX1, which encodes a monovalent cation/proton exchanger that traffics between the Golgi, endosomes, and vacuoles, also failed to rescue

and errors bars are the SD of three independent experiments. Unpaired t tests with Welch's correction were used to determine statistical significance; n.s., not significant; *, $P < 0.05$; **, $P < 0.01$; and ***, $P < 0.001$. Unless otherwise indicated, all other mutant strains were not statistically different compared with the wild-type control.

growth of *fab1Δ* yeast at 37°C (Supplemental Figure S7A). Moreover, whereas an *nhx1Δ* single mutant demonstrates a reduction in total potassium levels (Supplemental Figure S7B; Herrera et al., 2013), the *fab1Δnhx1Δ* double-mutant strain maintained a total potassium concentration nearly identical to that found in the *fab1Δ* parent strain (Supplemental Figure S7B). Although Nhx1, like Vnx1, is a monovalent cation/proton antiporter that mediates organellar cation import, Nhx1 loss of function might be ineffective toward rescuing the mutant phenotypes of *fab1Δ* yeast because the majority of Nhx1 localizes to the Golgi and endosomes, whereas Vnx1 localizes to the vacuole membrane (Supplemental Figure S7D; Ali et al., 2004).

The *vph1* and *vnx1* suppressor mutations relieve osmotic cellular swelling and cell lysis of *fab1Δ* yeast

Ppz1 and Ppz2 are protein phosphatases in yeast that negatively regulate the plasma membrane high-affinity potassium ion channels, Trk1 and Trk2. Thus, the *ppz1Δppz2Δ* strain accumulates high concentrations of intracellular potassium due to hyperactive potassium import across the plasma membrane (Yenush et al., 2002). We used the *ppz1Δppz2Δ* strain as a positive control in our ion content measurements and, indeed, found the *ppz1Δppz2Δ* strain demonstrated a robust accumulation of cellular potassium concentration to ~340 mM (Figure 5, A and B). Unlike *fab1Δ* cells, *ppz1Δppz2Δ* cells do not show an increase in sodium or calcium concentrations, demonstrating the specificity with which Ppz1 and Ppz2 regulate potassium ion transport (Figure 5, A and B).

The hyperactive import of potassium into *ppz1Δppz2Δ* cells causes osmotic cellular swelling, increased cell turgor, cell wall stress, and cell lysis at the nonpermissive temperature of 37°C (Figure 7, A and B; Yenush et al., 2002; Merchan et al., 2004). Because similar phenotypes are also exhibited by yeast deficient in PI(3,5)P₂ synthesis (Yamamoto et al., 1995), osmotic swelling of the vacuole might cause defects in the maintenance of cellular osmolarity. Supporting this idea, the growth of *fab1Δ* and *ppz1Δppz2Δ* cells at high temperature can be restored in the presence of an osmotic stabilizer, sorbitol (Figure 7A; Yamamoto et al., 1995; Yenush et al., 2002). The overall size of *fab1Δ* cells was reduced by the *vph1Δ* and *vnx1Δ* suppressor mutations, suggesting that loss of Vph1 or Vnx1 function not only reduces vacuole size but also relieves the defect in osmotic regulation caused by the loss of PI(3,5)P₂ signaling (Figure 7B). Unlike *fab1Δ* cells, removing *VPH1* or *VNX1* in *ppz1Δppz2Δ* cells (creating the triple mutants *ppz1Δppz2Δvph1Δ* and *ppz1Δppz2Δvnx1Δ*) did not recover growth at 37°C (Supplemental Figure 7E). This result was anticipated because Ppz1 and Ppz2 regulate potassium transport across the plasma membrane while Vph1 and Vnx1 regulate potassium transport across the vacuole membrane, and potassium transport at both sites is likely to be required for cells to buffer cytosolic levels of potassium.

Defective osmotic regulation in yeast can result in spontaneous cell lysis (Hughes et al., 1993; Merchan et al., 2004), which we observed for a proportion of *fab1Δ* and *ppz1Δppz2Δ* cells during their conversion to spheroplasts. Cellular lysis was indicated by the release of a cytosolic protein, Pgc1, into the surrounding buffer (Figure 7C). Unlike *fab1Δ* cells, we found that the release of Pgc1 is barely detectable upon converting wild-type, *vph1Δ*, or *vnx1Δ* yeast to spheroplasts (Figure 7, D and F). Doubling the osmotic support suppressed the spontaneous lysis phenotype of *fab1Δ* cells but not *ppz1Δppz2Δ* cells (Figure 7, D and E), consistent with our data that *ppz1Δppz2Δ* cells are larger and accumulate more potassium ions than *fab1Δ* cells (Figures 5B and 7B and Supplemental Figure 7C). Spontaneous lysis of *fab1Δ* cells was suppressed by the *vph1* and

vnx1 loss-of-function mutations (Figure 7F). Importantly, the cell lysis phenotype of *fab1Δ* yeast is not caused by poor growth or by general dysfunction of the endolysosomal pathway because the same lysis phenotype is not displayed by either *vps34Δ* or *doa4Δ* cells, which are two strains that are also temperature sensitive and have defects in the endolysosomal pathway (Figure 7F). Although the *vps34Δ* mutant strain lacks PI(3,5)P₂, it most likely presents a different spectrum of mutant phenotypes than does the *fab1Δ* strain because *vps34Δ* cells also lack PI3P, which is a phosphoinositide essential for normal endolysosomal membrane trafficking (Strahl and Thorner, 2007). Indeed, many *vps34Δ* cells have no identifiable endosomal or vacuolar structures, and unlike *fab1Δ* yeast, we measured a strong reduction in total potassium levels in *vps34Δ* cells (Supplemental Figure 7, B and C). Intriguingly, a *fab1Δvps34Δ* strain grows much slower than the *vps34Δ* or *fab1Δ* single mutants and lyses upon conversion to spheroplasts, suggesting that the Fab1 protein performs additional roles in maintaining cellular homeostasis other than synthesizing PI(3,5)P₂ (Figure 7F).

DISCUSSION

The low-abundant phosphoinositide PI(3,5)P₂ is distinguished as an essential controller of lysosome morphology and function (McCartney et al., 2014). An emerging role for PI(3,5)P₂ signaling at lysosomes is the regulation of ion transport by modulating the activity of lysosomal ion transporters and channels (Dong et al., 2010; Wang et al., 2012; Carpaneto et al., 2017). The rapid directional transport of ions across cellular membranes is known to participate in cell signaling pathways and invoke morphological changes in organelles, suggesting that PI(3,5)P₂ may act, in part, to control lysosome function by regulating multiple ion transport systems at lysosomes (Scott and Gruenberg, 2011; Barragán et al., 2012). The scope of ions or metabolites mobilized by a PI(3,5)P₂ signaling event, however, is not well understood, nor is the cohort of transporters/channels regulated by PI(3,5)P₂ or the purpose of this regulation.

The phosphorylation of PI3P by Fab1 is the only route to synthesize PI(3,5)P₂ in *S. cerevisiae* (Gary et al., 1998). Yeast lacking *FAB1* contain grossly enlarged vacuoles and exhibit severe growth defects (Yamamoto et al., 1995). Our unbiased screen for suppressor mutations that relieve the growth defect of *fab1Δ* cells identified loss-of-function mutations in *Vph1* and *Vnx1*. Importantly, we confirmed in multiple genetic backgrounds that disruption of *Vph1* or *Vnx1* function strongly and specifically enhances the growth of yeast deficient in PI(3,5)P₂ signaling. Prompted by the genetic relationship between *FAB1*, *VPH1*, and *VNX1*, we found that *fab1Δ* yeast exhibit increases in potassium, calcium, and sodium concentrations. In *fab1Δ* yeast, the ~85 mM increase in potassium (vs. 0.7 and 3.8 mM increases in calcium and sodium, respectively) is consistent with potassium being the relevant osmolyte among these cations accumulated in PI(3,5)P₂-deficient yeast. Disabling the functions of other transporters known to facilitate vacuolar/endosomal import of cations (*Vcx1*, *Nhx1*, and *Pmc1*; Pozos et al., 1996; Nass et al., 1997) failed to recover the growth of *fab1Δ* cells. These findings are consistent with the report that *Vnx1* is the primary transporter that imports potassium into the vacuole lumen (Cagnac et al., 2007). In total, our data point to a role for PI(3,5)P₂ in regulating potassium storage within yeast vacuoles in order to mediate changes in vacuole morphology and maintain cellular osmoregulation.

In yeast, PI(3,5)P₂ levels rapidly climb ~20-fold within 15 min after hyperosmotic shock and then return to baseline levels (Dove et al., 1997; Duex et al., 2006). Mirroring this temporal activation of PI(3,5)P₂ synthesis, vacuoles transiently fragment and release cations within 15 min after hyperosmotic shock (Denis and Cyert, 2002;

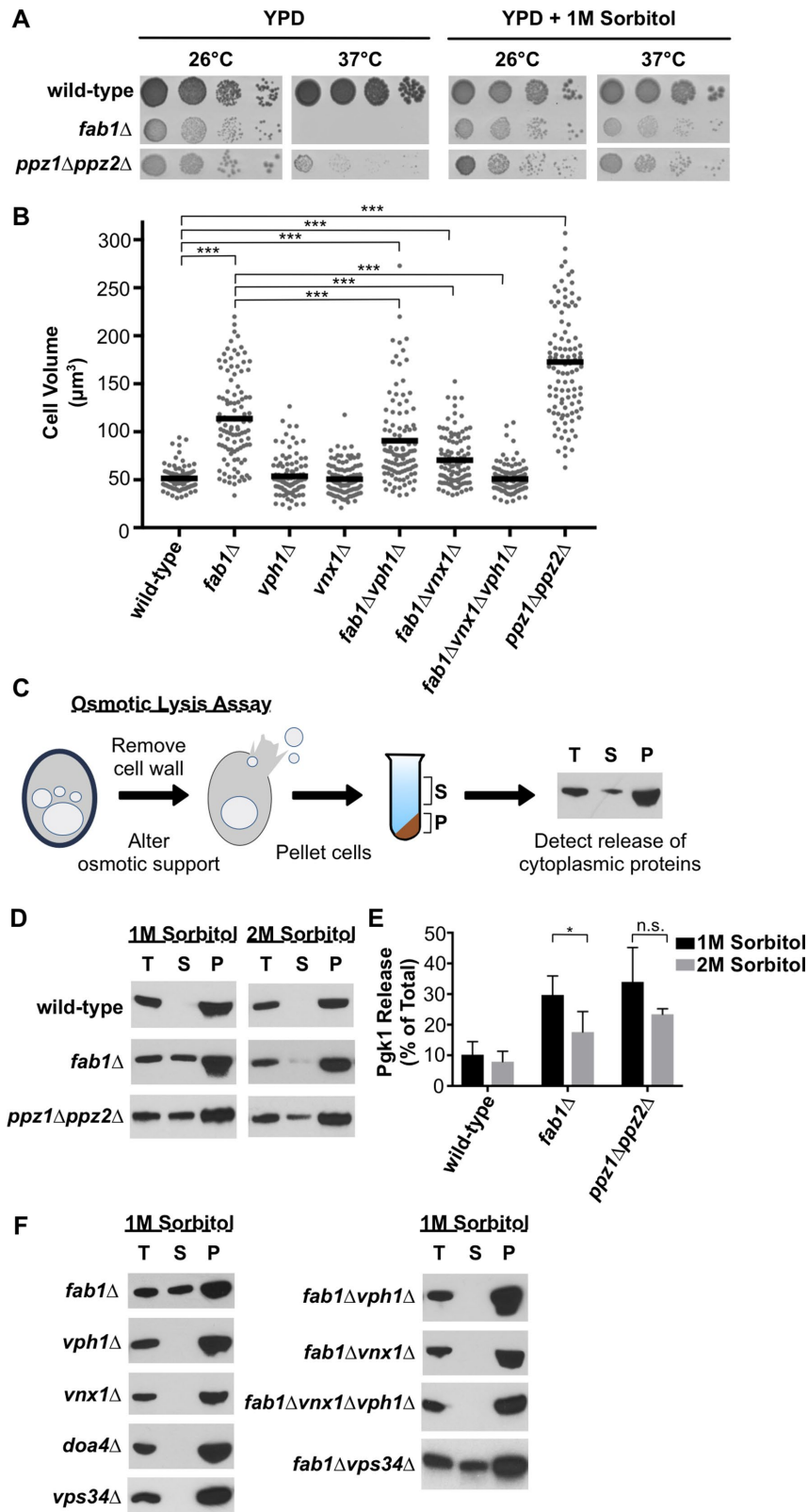


FIGURE 7: Suppressor mutations relieve osmotic swelling and cell lysis of *fab1*Δ yeast. (A) Cell growth assay of the indicated yeast strains grown on rich agar medium (YPD) in the absence or presence of 1 M sorbitol at 26°C or 37°C for 3 d. (B) Quantitation of cell volume measurements of the indicated strains. Each dot represents a single cell, with the horizontal line representing the mean of all measurements ($n > 100$ per strain). Unpaired t tests with Welch's correction were used to determine statistical significance; ***, $P < 0.001$. Unless otherwise indicated, all other mutant strains were not statistically

Duex *et al.*, 2006). This dramatic reduction in vacuolar volume requires the activation of vacuole fission, inhibition of vacuole fusion, and the efficient release of vacuolar content. Considering yeast cells store high concentrations of potassium, with a large proportion (~50%) of this potassium pool held within the vacuole (Herrera *et al.*, 2013), the regulated transport of potassium is expected to facilitate these changes in vacuole morphology. Although less is known about potassium transport at the yeast vacuole, potassium transport at plant vacuoles has a fundamental role in regulating vacuole morphology and cellular osmoregulation (Barragán *et al.*, 2012). For example, vacuolar import of potassium by antiporters similar to Vnx1 induces osmotic swelling of guard cell vacuoles to increase cell turgor pressure and open stoma for transpiration (Barragán *et al.*, 2012; Andrés *et al.*, 2014).

How could PI(3,5)P₂ regulate potassium transport at the vacuole? One route appears to be via the yeast vacuolar cation export channel, Yvc1, which is activated by hyperosmotic stress in a manner that depends upon PI(3,5)P₂ signaling (Denis and Cyert, 2002; Dong *et al.*, 2010). Studies of Yvc1 have primarily focused on calcium signaling, but this general cation export channel has also been proposed to release potassium from vacuoles in response to hyperosmotic stress (Bertl and Slayman, 1990; Palmer *et al.*, 2001; Chang *et al.*, 2010). Indeed, we found that overexpression of the Yvc1 gain-of-function mutant protein, Yvc1^{Y458H}, reduced the levels of sodium, potassium, and calcium in *fab1*Δ yeast. Notably, we found that cells lacking Yvc1 function do not

different compared with the wild-type control. (C) Cartoon depiction of osmotic lysis assay. The total (T), pellet (P), and supernatant (S) were analyzed by Western blot, probing for the cytosolic protein Pgk1. Appearance of Pgk1 in the supernatant indicates cell lysis during spheroplast conversion. (D) Osmotic lysis assay as described in C of wild-type, *fab1*Δ, or *ppz1*Δ*ppz2*Δ yeast in the presence of 1 or 2 M sorbitol in the buffer. The inability to block the cell lysis of *ppz1*Δ*ppz2*Δ cells also confirms that increasing osmotic support does not inhibit the conversion of cells into spheroplasts. Shown are representative blots of three independent experiments. (E) Quantitation of Pgk1 release of the experiment performed in D. Pgk1 release is determined as a percentage of Pgk1 detected in the supernatant compared with the total Pgk1 detected in the supernatant and pellet. Bars represent the mean and errors bars are the SD of three independent experiments. Unpaired t tests with Welch's correction were used to determine statistical significance; n.s., not significant; *, $P < 0.05$. (F) Osmotic lysis assay as described in C and D of the indicated yeast strains. Shown are representative blots of two independent experiments.

phenocopy the vacuole enlargement or cation accumulation seen in *fab1Δ* cells. Therefore, Yvc1 is unlikely to be the only means by which PI(3,5)P₂ regulates vacuolar/cellular osmolarity.

Our finding that a *vnx1Δ* mutation suppresses the phenotypes caused by the loss of Fab1 activity suggest that a major route by which PI(3,5)P₂ regulates vacuolar potassium transport is through negative regulation of Vnx1. PI(3,5)P₂ could control Vnx1 function indirectly by recruiting a regulatory protein to the vacuole membrane or through calcium signaling by increasing cytosolic calcium levels via the activation of Yvc1. Alternatively, Vnx1 could be a direct target of PI(3,5)P₂ signaling. Transporters and channels shown to be regulated directly by phosphoinositides have a cytosolic domain that contains polybasic regions rich in arginine and lysine residues, which interact with negatively charged phosphoinositide head groups (Nilius *et al.*, 2008; Suh and Hille, 2008). Similarly, Vnx1 has a large N-terminal cytosolic domain with polybasic regions, but whether this domain binds PI(3,5)P₂ or regulates Vnx1 function has yet to be determined.

Our results, in combination with previous reports, suggest a model in which the elevation of PI(3,5)P₂ levels induced by hyperosmotic stress activates Yvc1 and simultaneously inhibits Vnx1, thereby promoting the release of vacuolar cation stores (Dove *et al.*, 1997; Denis and Cyert, 2002; Duex *et al.*, 2006; Dong *et al.*, 2010). Releasing vacuolar cations to the cytosol is predicted to reduce cellular water loss, prevent ion toxicity, and—in the case of calcium—induce cell-stress signaling pathways that aid the adaptive response to acute hyperosmotic stress (Munns and Tester, 2008; Cunningham, 2011). Accordingly, PI(3,5)P₂ deficiency is expected to inhibit Yvc1 activity and promote Vnx1 function to increase the storage of potassium (and other cations) in the vacuole, which draws water in from the cytoplasm. Whether PI(3,5)P₂ levels drop during hypoosmotic shock to promote vacuole expansion and water absorption remains to be tested.

Regulation of vacuolar/lysosomal ion storage by PI(3,5)P₂ is likely to be conserved. A phenotype common to all organisms in which PI(3,5)P₂ signaling has been disrupted is the dramatic swelling of endolysosomal organelles (Gary *et al.*, 1998; Ikononov *et al.*, 2001; Nicot *et al.*, 2006; Rusten *et al.*, 2006). At least part of this organellar expansion is caused by osmotic swelling because vacuoles/lysosomes in PI(3,5)P₂-deficient cells are much larger than vacuoles/lysosomes that are enlarged as a result of defective membrane fission (Bonangelino *et al.*, 2002; Dove *et al.*, 2004). A conserved role for PI(3,5)P₂ signaling in regulating lysosomal ion homeostasis is supported by evidence that PI(3,5)P₂ activates multiple lysosomal cation export channels, including TRPML1 and lysosomal two-pore channels (Dong *et al.*, 2010; Wang *et al.*, 2012). Although there is currently no evidence that PI(3,5)P₂ regulates cation antiporters at the lysosome membrane, several plasma membrane cation antiporters in metazoans are regulated by phosphatidylinositol-4,5-bisphosphate (Hilgemann and Ball, 1996; Suh and Hille, 2008), providing the rationale that PI(3,5)P₂-regulated cation antiporters exist. Supporting the idea that PI(3,5)P₂ regulates the import of specific ions or metabolites into vacuoles/lysosomes, a recent study showed that PI(3,5)P₂ inhibits a Cl⁻/H⁺ antiporter at plant vacuoles (Carpaneto *et al.*, 2017). Furthermore, the lysosomal enlargement phenotype of mammalian cells with depleted PI(3,5)P₂ levels can be suppressed by pharmacological inhibition of V-ATPase function, consistent with our results (Compton *et al.*, 2016).

Our identification of loss-of-function mutations in *VPH1* as suppressor mutations of *fab1Δ* yeast can be interpreted on the basis that disruption of the vacuole proton gradient blocks the hyperactive import of potassium and other osmolytes into the vacuole

lumen. This idea is also supported by the observation that the V-ATPase inhibitor, bafilomycin-A1, inhibits vacuole enlargement in *fab1^{ts}* cells shifted to the nonpermissive temperature of 37°C. Interestingly, combining the *vph1* and *vnx1* suppressor mutations recovered normal vacuole and cell size in *fab1Δ* cells more strongly than did either suppressor mutation alone. This synthetic suppressive effect could result from enhanced vacuolar fragmentation, as V-ATPase activity is required for homotypic vacuole fusion (Baars *et al.*, 2007). Alternatively, this result may signify that the vacuolar import of ions and metabolites other than just monovalent cations are regulated by PI(3,5)P₂ signaling.

Fab1 function is regulated by Pho80-Pho85, a cyclin/cyclin-dependent kinase complex that is best known for regulating the phosphate-sensing and metabolism pathway (Carroll and O'Shea 2002; Jin *et al.*, 2017). It is intriguing that we observed a decrease in total phosphorous levels in *fab1Δ* cells, suggesting that vacuoles in yeast lacking PI(3,5)P₂ may store less polyphosphate. PI(3,5)P₂ signaling might, therefore, regulate polyphosphate synthesis or phosphate mobilization from the vacuole to buffer cytosolic pools of phosphate. Because polyphosphate levels play a critical role in regulating vacuolar osmolarity by complexing with cations within the vacuole lumen (Dunn *et al.*, 1994; Beeler *et al.*, 1997), the decrease in phosphorous levels we observed in *fab1Δ* cells may be among the pleiotropic causes that induce vacuole enlargement.

MATERIALS AND METHODS

Yeast strains and plasmid construction

All strains and plasmids used in this study are listed in Supplemental Tables 1 and 2, respectively. Genetic disruptions were constructed through homologous recombination of integration cassettes described in Longtine *et al.* (1998) or Gauss *et al.* (2005). To generate a plasmid expressing Vph1, the *VPH1* locus, including ~500 base pairs of both the 5'-UTR and 3'-UTR, was amplified using primers that contained 5'-overhangs that anneal within the multiple cloning site of the low-copy number (CEN) pRS416 vector, allowing for homologous recombination of *VPH1* into an *EcoRI*-cut pRS416 vector in yeast. The plasmid pZW16, containing the *VNX1* locus, was generated in the same manner as described for *VPH1* but recombined into a *SacI*-cut pRS416 vector. To create an integrated *vph1^{R735Q}* mutant, the previously cloned *VPH1* locus was ligated into pRS306 and mutated following the QuikChange Site-Directed Mutagenesis Kit protocol using the following primers: 5'-CGCACACTGCATCCTATTACAGTTATGGCCTTATCATTGGC-3' and 5'-GCCAATGATAAGGCCATAACTGTAAATAGGATGCAGTGTGCG-3' (Stratagene 2006). Sequencing confirmed the amino acid change, and the plasmid was named pZW10. pZW10 was cut by *BspEI* and integrated into *fab1Δ* yeast using standard techniques. To remove the *URA3* cassette, integrants were plated onto minimal synthetic medium (YNB) containing 0.1% (wt/vol) 5-fluoroorotic acid as a counterselection. Construction of an integrated *vph1^{R735Q}* mutant was confirmed by sequencing of clones that survived counterselection. All *Sna3*-pHluorin integrations were constructed following the same procedure outlined in Prosser *et al.* (2010).

Yeast media and growth

All yeast strains were grown at 26°C unless stated otherwise. Yeast were grown in either YPD (1% yeast extract, 2% peptone, 2% dextrose) medium or minimal synthetic medium (YNB) lacking the appropriate nutrient for selection. Yeast strains containing *URA3* or *TRP1* plasmids were grown in YNB-Ura or YNB-Trp supplemented with 0.10% (wt/vol) casamino acids. For plate-spotting assays, yeast cultures were grown to mid-log phase, set to the same density

(1 OD₆₀₀/ml), and serially diluted 10-fold, and cells (~5 µl) were spotted onto growth medium.

Identifying suppressors of *fab1Δ* yeast

Suppressors of *fab1Δ* yeast were isolated by serially diluting mid-log-phase yeast and plating onto YPD agar at 37°C. Clonal isolates were catalogued *fab1Δbfo#* for Bypass Fab1. To identify the suppressing mutations, *fab1Δbfo* suppressors were mated to the *fab1Δ* Mat, a parent strain to obtain diploids homozygous for *fab1Δ* and heterozygous for the suppressing mutation. Subsequent sporulation of diploids produced *fab1Δbfo* mutants in both Mat α and “a” strains, allowing for standard genetic complementation assays to be performed. To identify potential suppressing mutations, representative mutants from the complementation groups and the wild-type SEY6210 parent strain were whole-genome sequenced following procedures similar to those described in Selmecki *et al.* (2015). Briefly, whole-genome sequences were mapped to an S288C reference genome, and candidate suppressor mutations were identified by performing a variant-calling analysis using Genome Analysis Toolkit UnifiedGenotyper (version 2.4-9; McKenna *et al.*, 2010; Selmecki *et al.*, 2015). Putative suppressor mutations were identified as variants that occurred in a suppressor strain but were not present within the wild-type SEY6210 parent or the other representative suppressor strain.

Fluorescence microscopy

Yeast were labeled with FM 4-64 (Life Technologies, Carlsbad, CA) following a pulse-chase procedure that has been previously described (Shideler *et al.*, 2015). Briefly, 1 ml of mid-log-phase cells were suspended in YPD medium containing 1.6 µM FM 4-64 for 20 min at 30°C, then placed in 5 ml of YPD medium at 26°C for a 90-min chase period in the absence of FM 4-64 before microscopy. For the bafilomycin-A1 experiments, yeast were labeled with FM 4-64 as described but were allowed to chase in YPD medium for only 30 min. Subsequently, cells were placed in a small volume of minimal synthetic medium containing all required nutrients (YNB complete) that contained either dimethyl sulfoxide (DMSO; vehicle control) or 10 µM bafilomycin-A1 (Sigma-Aldrich). After incubating at 26°C or 37°C for 2 h the cells were visualized by confocal fluorescence microscopy. Confocal fluorescence microscopy was performed using an inverted fluorescence microscope (TE2000-U; Nikon, Melville, NY) equipped with a 100x/numerical aperture 1.4 oil objective and a Yokogawa spinning disk confocal system (CSU-Xm2; Nikon). Images were taken using a Photometrics (Tucson, AZ) Cascade II EM-CCD camera, acquired with Metamorph version 7.0 software (MDS Analytical Technologies, Sunnyvale, CA), and analyzed using either ImageJ software (National Institutes of Health, Bethesda, MD) or Photoshop CS5 (Adobe Systems, San Jose, CA).

Osmotic lysis assay of yeast spheroplasts

Aberrant cell lysis was determined by converting yeast to spheroplasts following a standard procedure and detecting lysis by release of the cytosolic protein, Pgk1, by Western blotting. Briefly, 5 OD₆₀₀ equivalents of exponentially growing yeast were collected, washed once in sterile water, and incubated for 15 min in softening buffer (100 mM HEPES, pH 9.4, 10 mM dithiothreitol). The softening buffer was removed, and cells were suspended in spheroplasting buffer (YNB media containing 100 mM HEPES, pH 7.4, and 1 or 2 M sorbitol) and incubated at 30°C with Zymolase 20T (MP Biomedicals, Santa Ana, CA) for 90 min. One OD₆₀₀ equivalent was removed as the total, and spheroplasts were pelleted at 5000 × g for 10 min. The supernatant was removed, and the spheroplasts were suspended in

water, providing a check for spheroplast conversion based on lysis in water. The total, supernatant, and spheroplast (pellet) fractions were precipitated in 10% (vol/vol) trichloroacetic acid. The precipitant was washed thrice in ice-cold acetone before being suspended in Laemmli buffer. Samples were boiled at 95°C before being resolved by SDS-PAGE in 10% acrylamide (vol/vol) Tris/glycine gels. Proteins were then transferred to a nitrocellulose membrane and treated with anti-PGK monoclonal antibody (ThermoFisher Scientific, Waltham, MA). Primary antibodies were detected using a goat anti-mouse horseradish peroxidase-conjugated secondary antibody (Santa Cruz Biotechnology, Dallas, TX) that allowed for chemiluminescence detection using autoradiography film or using goat anti-mouse Cy3-conjugated secondary antibody (GE Healthcare, Marlborough, MA) that allowed for fluorescence detection and quantitation using a Typhoon FLA 9500 biomolecular imager (GE Healthcare).

Measuring ion content by ICP-AES

The ion content of yeast was determined by inductively coupled plasma atomic emission spectroscopy (ICP-AES) at the Laboratory of Geological Studies (LEGS) at the University of Colorado Boulder. Preparation of cell samples for ICP-AES was performed similar to that described in Eide *et al.* (2005) with minor modifications. Sixty OD₆₀₀ equivalents of exponentially growing cells in YPD medium were collected 15 ODs at a time by vacuum filtration onto isopore membranes (1.2 µm pore size; Fisher Scientific, Hampton, NH). Cells were washed twice with 5 ml, 1 M sorbitol containing 1 µM EDTA and then twice more with 5 ml, 1 M sorbitol. Following washes, two filters with 15 ODs of cells were combined into a screw-top microcentrifuge tube and dissolved in 500 µl 30% nitric acid at 65°C overnight. After acid digestion, the filters were removed and two 500-µl samples were combined into one tube and centrifuged at 12,000 × g to pellet any debris. Approximately 55 OD₆₀₀ equivalents of cell digests were diluted in 4.1 ml sterile Ultra Pure water (Fisher Scientific, Hampton, NH) and submitted for ICP-AES analysis. Each experiment included two technical replicates and a buffer-only control to normalize for ion contaminants provided by the YPD media, wash buffers, nitric acid, or water used in the analysis. Determination of atoms/cell or ion concentrations were based, respectively, on the average cell number counted per 1 OD₆₀₀ by a hemacytometer or the average cell volume determined by measuring the cell diameter of each strain by fluorescence microscopy, assuming a spherical cell shape. Wild-type and *fab1Δ* yeast expressing *YVC1* or *ycv1^{Y458H}* from the high-copy number (2µ) pRS424 expression vector were grown overnight in YNB-Trp media, then diluted to 0.1–0.2 OD₆₀₀ in YPD and collected at 0.8–1 OD₆₀₀ to standardize ion content measurements with wild-type yeast and knockout strains performed in YPD media.

ACKNOWLEDGMENTS

We thank Ian McKittrick (University of Colorado) for genetic analysis of mutant strains, Phillip Richmond (University of Colorado) for genome sequence mapping and variant analysis, and Fred Luiszer at the LEGS facility at the University of Colorado for performing ICP-AES. We thank Tom Stevens (University of Oregon), Alexey Merz (University of Washington), and Scott Emr (Cornell University) for plasmids and/or yeast strains. We thank Dalton Buysse (University of Colorado) for plasmid and yeast strain constructions, for helpful discussions, and for critical reading of the manuscript. This work was funded by National Institutes of Health Grant no. R01GM-111335 to G.O., by a University of Colorado Boulder Innovation Seed Grant to G.O., and by National Science Foundation GRFP Award No. DGE-1144083 to Z.W.

REFERENCES

- Ali R, Brett CL, Mukherjee S, Rao R (2004). Inhibition of sodium/proton exchange by a Rab-GTPase-activating protein regulates endosomal traffic in yeast. *J Biol Chem* 279, 4498–4506.
- Andrés Z, Pérez-Hormaeche J, Leidi EO, Schlücking K, Steinhorst L, McLachlan DH, Schumacher K, Hetherington AM, Kudla J, Cubero B, Pardo JM (2014). Control of vacuolar dynamics and regulation of stomatal aperture by tonoplast potassium uptake. *Proc Natl Acad Sci USA* 111, E1806–E1814.
- Ariño J, Ramos J, Sychrová H (2010). Alkali metal cation transport and homeostasis in yeasts. *Microbiol Mol Biol Rev* 74, 95–120.
- Baars TL, Petri S, Peters C, Mayer A (2007). Role of the V-ATPase in regulation of the vacuolar fission-fusion equilibrium. *Mol Biol Cell* 18, 3873–3882.
- Barragán V, Leidi EO, Andrés Z, Rubio L, De Luca A, Fernández JA, Cubero B, Pardo JM (2012). Ion exchangers NHX1 and NHX2 mediate active potassium uptake into vacuoles to regulate cell turgor and stomatal function in *Arabidopsis*. *Plant Cell* 24, 1127–1142.
- Beeler T, Bruce K, Dunn T (1997). Regulation of cellular Mg²⁺ by *Saccharomyces cerevisiae*. *Biochim Biophys Acta* 1323, 310–318.
- Bertl A, Slayman CL (1990). Cation-selective channels in the vacuolar membrane of *Saccharomyces*: dependence on calcium, redox state, and voltage. *Proc Natl Acad Sci USA* 87, 7824–7828.
- Bonangelino CJ, Nau JJ, Duex JE, Brinkman M, Wurmsler AE, Gary JD, Emr SD, Weisman LS (2002). Osmotic stress-induced increase of phosphatidylinositol 3,5-bisphosphate requires Vac14p, an activator of the lipid kinase Fab1p. *J Cell Biol* 156, 1015–1028.
- Cagnac O, Leterrier M, Yeager M, Blumwald E (2007). Identification and characterization of Vnx1p, a novel type of vacuolar monovalent cation/H⁺ antiporter of *Saccharomyces cerevisiae*. *J Biol Chem* 282, 24284–24293.
- Carpaneto A, Boccaccio A, Lagostena L, Di Zanni E, Scholz-Starke J (2017). The signaling lipid phosphatidylinositol-3,5-bisphosphate targets plant CLC-a anion/H⁺ exchange activity. *EMBO Rep* 18, 1100–1107.
- Carroll AS, O'Shea EK (2002). Pho85 and signaling environmental conditions. *Trends Biochem Sci* 27, 87–93.
- Castrol CD, Koretsky AP, Domach MM (1999). NMR-observed phosphate trafficking and polyphosphate dynamics in wild-type and vph1-1 mutant *Saccharomyces cerevisiae* in response to stresses. *Biotechnol Prog* 15, 65–73.
- Chang Y, Schlenstedt G, Flockerzi V, Beck A (2010). Properties of the intracellular transient receptor potential (TRP) channel in yeast, Yvc1. *FEBS Lett* 584, 2028–2032.
- Compton LM, Ikononov OC, Sbrissa D, Garg P, Shisheva A (2016). Active vacuolar H⁺ ATPase and functional cycle of Rab5 are required for the vacuolation defect triggered by PtdIns(3,5)P₂ loss under PIKfyve or Vps34 deficiency. *Am J Physiol Cell Physiol* 311, C366–C377.
- Coonrod EM, Graham LA, Carpp LN, Carr TM, Stirrat L, Bowers K, Bryant NJ, Stevens TH (2013). Homotypic vacuole fusion in yeast requires organelle acidification and not the V-ATPase membrane domain. *Dev Cell* 27, 462–468.
- Cunningham KW (2011). Acidic calcium stores of *Saccharomyces cerevisiae*. *Cell Calcium* 50, 129–138.
- Denis V, Cyert MS (2002). Internal Ca²⁺ release in yeast is triggered by hypertonic shock and mediated by a TRP channel homologue. *J Cell Biol* 156, 29–34.
- Dong X-P, Shen D, Wang X, Dawson T, Li X, Zhang Q, Cheng X, Zhang Y, Weisman LS, Dellling M, Xu H (2010). PI(3,5)P₂ controls membrane trafficking by direct activation of mucolipin Ca²⁺ release channels in the endolysosome. *Nat Commun* 1, 38.
- Dove SK, Cooke FT, Douglas MR, Sayers LG, Parker PJ, Michell RH (1997). Osmotic stress activates phosphatidylinositol-3,5-bisphosphate synthesis. *Nature* 390, 187–192.
- Dove SK, Piper RC, McEwen RK, Yu JW, King MC, Hughes DC, Thuring J, Holmes AB, Cooke FT, Michell RH, et al. (2004). Svp1p defines a family of phosphatidylinositol 3,5-bisphosphate effectors. *EMBO J* 23, 1922–1933.
- Duex JE, Nau JJ, Kauffman EJ, Weisman LS (2006). Phosphoinositide 5-phosphatase Fig4p is required for both acute rise and subsequent fall in stress-induced phosphatidylinositol 3,5-bisphosphate levels. *Eukaryotic Cell* 5, 723–731.
- Dunn T, Gable K, Beeler T (1994). Regulation of cellular Ca²⁺ by yeast vacuoles. *J Biol Chem* 269, 7273–7278.
- Eide DJ, Clark S, Nair TM, Gehl M, Gribskov M, Guerinot ML, Harper JF (2005). Characterization of the yeast ionome: a genome-wide analysis of nutrient mineral and trace element homeostasis in *Saccharomyces cerevisiae*. *Genome Biol* 6, R77.
- Finnigan GC, Cronan GE, Park HJ, Srinivasan S, Quioco FA, Stevens TH (2012). Sorting of the yeast vacuolar-type, proton-translocating ATPase enzyme complex (V-ATPase): identification of a necessary and sufficient Golgi/endosomal retention signal in Stv1p. *J Biol Chem* 287, 19487–19500.
- Gary JD, Sato TK, Stefan CJ, Bonangelino CJ, Weisman LS, Emr SD (2002). Regulation of Fab1 phosphatidylinositol 3-phosphate 5-kinase pathway by Vac7 protein and Fig4, a polyphosphoinositide phosphatase family member. *Mol Biol Cell* 13, 1238–1251.
- Gary JD, Wurmsler AE, Bonangelino CJ, Weisman LS, Emr SD (1998). Fab1p is essential for PtdIns(3)P 5-kinase activity and the maintenance of vacuolar size and membrane homeostasis. *J Cell Biol* 143, 65–79.
- Gauss R, Trautwein M, Sommer T, Spang A (2005). New modules for the repeated internal and N-terminal epitope tagging of genes in *Saccharomyces cerevisiae*. *Yeast* 22, 1–12.
- Herrera R, Álvarez MC, Gelis S, Ramos J (2013). Subcellular potassium and sodium distribution in *Saccharomyces cerevisiae* wild-type and vacuolar mutants. *Biochem J* 454, 525–532.
- Hilgemann DW, Ball R (1996). Regulation of cardiac Na⁺,Ca²⁺ exchange and K_{ATP} potassium channels by PIP₂. *Science* 273, 956–959.
- Ho CY, Choy CH, Wattson CA, Johnson DE, Botelho RJ (2015). The Fab1/PIKfyve phosphoinositide phosphate kinase is not necessary to maintain the pH of lysosomes and of the yeast vacuole. *J Biol Chem* 290, 9919–9928.
- Hughes V, Müller A, Stark MJ, Cohen PT (1993). Both isoforms of protein phosphatase Z are essential for the maintenance of cell size and integrity in *Saccharomyces cerevisiae* in response to osmotic stress. *Eur J Biochem* 216, 269–279.
- Ikononov OC, Sbrissa D, Shisheva A (2001). Mammalian cell morphology and endocytic membrane homeostasis require enzymatically active phosphoinositide 5-kinase PIKfyve. *J Biol Chem* 276, 26141–26147.
- Jin N, Chow CY, Liu L, Zolov SN, Bronson R, Davisson M, Petersen JL, Zhang Y, Park S, Duex JE, et al. (2008). VAC14 nucleates a protein complex essential for the acute interconversion of PI3P and PI(3,5)P₂ in yeast and mouse. *EMBO J* 27, 3221–3234.
- Jin N, Jin Y, Weisman LS (2017). Early protection to stress mediated by CDK-dependent PI3,5P₂ signaling from the vacuole/lysosome. *J Cell Biol* 216, 2075–2090.
- Kane PM (2006). The where, when, and how of organelle acidification by the yeast vacuolar H⁺-ATPase. *Microbiol Mol Biol Rev* 70, 177–191.
- Kawasaki-Nishi S, Nishi T, Forgac M (2001). Arg-735 of the 100-kDa subunit a of the yeast V-ATPase is essential for proton translocation. *Proc Natl Acad Sci USA* 98, 12397–12402.
- Li SC, Diakov TT, Xu T, Tarsio M, Zhu W, Couoh-Cardel S, Weisman LS, Kane PM (2014). The signaling lipid PI(3,5)P₂ stabilizes V₂–V₆ sector interactions and activates the V-ATPase. *Mol Biol Cell* 25, 1251–1262.
- Li SC, Kane PM (2009). The yeast lysosome-like vacuole: endpoint and crossroads. *Biochim Biophys Acta* 1793, 650–663.
- Longtine MS, McKenzie A, Demarini DJ, Shah NG, Wach A, Brachat A, Philippsen P, Pringle JR (1998). Additional modules for versatile and economical PCR-based gene deletion and modification in *Saccharomyces cerevisiae*. *Yeast* 14, 953–961.
- McCartney AJ, Zhang Y, Weisman LS (2014). Phosphatidylinositol 3,5-bisphosphate: low abundance, high significance. *Bioessays* 36, 52–64.
- McKenna A, Hanna M, Banks E, Sivachenko A, Cibulskis K, Kernytsky A, Garimella K, Altshuler D, Gabriel S, Daly M, DePristo MA (2010). The Genome Analysis Toolkit: a MapReduce framework for analyzing next-generation DNA sequencing data. *Genome Res* 20, 1297–1303.
- Merchan S, Bernal D, Serrano R, Yenush L (2004). Response of the *Saccharomyces cerevisiae* Mpk1 mitogen-activated protein kinase pathway to increases in internal turgor pressure caused by loss of Ppz protein phosphatases. *Eukaryot Cell* 3, 100–107.
- Munns R, Tester M (2008). Mechanisms of salinity tolerance. *Annu Rev Plant Biol* 59, 651–681.
- Nass R, Cunningham KW, Rao R (1997). Intracellular sequestration of sodium by a novel Na⁺/H⁺ exchanger in yeast is enhanced by mutations in the plasma membrane H⁺-ATPase. Insights into mechanisms of sodium tolerance. *J Biol Chem* 272, 26145–26152.
- Nicot A-S, Fares H, Payrastra B, Chisholm AD, Labouesse M, Laporte J (2006). The phosphoinositide kinase PIKfyve/Fab1p regulates terminal lysosome maturation in *Caenorhabditis elegans*. *Mol Biol Cell* 17, 3062–3074.

- Nilius B, Owsianik G, Voets T (2008). Transient receptor potential channels meet phosphoinositides. *EMBO J* 27, 2809–2816.
- Palmer CP, Zhou XL, Lin J, Loukin SH, Kung C, Saimi Y (2001). A TRP homolog in *Saccharomyces cerevisiae* forms an intracellular Ca²⁺-permeable channel in the yeast vacuolar membrane. *Proc Natl Acad Sci USA* 98, 7801–7805.
- Pozos TC, Sekler I, Cyert MS (1996). The product of HUM1, a novel yeast gene, is required for vacuolar Ca²⁺/H⁺ exchange and is related to mammalian Na⁺/Ca²⁺ exchangers. *Mol Cell Biol* 16, 3730–3741.
- Prosser DC, Whitworth K, Wendland B (2010). Quantitative analysis of endocytosis with cytoplasmic pHluorin chimeras. *Traffic* 11, 1141–1150.
- Qiu Q-S, Fratti RA (2010). The Na⁺/H⁺ exchanger Nhx1p regulates the initiation of *Saccharomyces cerevisiae* vacuole fusion. *J Cell Sci* 123, 3266–3275.
- Rohacs T (2009). Phosphoinositide regulation of non-canonical transient receptor potential channels. *Cell Calcium* 45, 554–565.
- Rusten TE, Rodahl LMW, Pattni K, Englund C, Samakovlis C, Dove S, Brech A, Stenmark H (2006). Fab1 phosphatidylinositol 3-phosphate 5-kinase controls trafficking but not silencing of endocytosed receptors. *Mol Biol Cell* 17, 3989–4001.
- Sankaranarayanan S, De Angelis D, Rothman JE, Ryan TA (2000). The use of pHluorins for optical measurements of presynaptic activity. *Biophys J* 79, 2199–2208.
- Sbrissa D, Ikononov OC, Fu Z, Ijuin T, Gruenberg J, Takenawa T, Shisheva A (2007). Core protein machinery for mammalian phosphatidylinositol 3,5-bisphosphate synthesis and turnover that regulates the progression of endosomal transport. Novel Sac phosphatase joins the ArPIKfyve-PIKfyve complex. *J Biol Chem* 282, 23878–23891.
- Sbrissa D, Ikononov OC, Shisheva A (1999). PIKfyve, a mammalian ortholog of yeast Fab1p lipid kinase, synthesizes 5-phosphoinositides. Effect of insulin. *J Biol Chem* 274, 21589–21597.
- Scott CC, Gruenberg J (2011). Ion flux and the function of endosomes and lysosomes: pH is just the start. The flux of ions across endosomal membranes influences endosome function not only through regulation of the luminal pH. *Bioessays* 33, 103–110.
- Selmecki AM, Maruvka YE, Richmond PA, Guillet M, Shoresh N, Sorenson AL, De S, Kishony R, Michor F, Dowell R, Pellman D (2015). Polyploidy can drive rapid adaptation in yeast. *Nature* 519, 349–352.
- Shideler T, Nickerson DP, Merz AJ, Odorizzi G (2015). Ubiquitin binding by the CUE domain promotes endosomal localization of the Rab5 GEF Vps9. *Mol Biol Cell* 26, 1345–1356.
- Smardon AM, Diab HI, Tarsio M, Diakov TT, Nasab ND, West RW, Kane PM (2014). The RAVE complex is an isoform-specific V-ATPase assembly factor in yeast. *Mol Biol Cell* 25, 356–367.
- Strahl T, Thorner J (2007). Synthesis and function of membrane phosphoinositides in budding yeast, *Saccharomyces cerevisiae*. *Biochim Biophys Acta* 1771, 353–404.
- Suh B-C, Hille B (2008). PIP2 is a necessary cofactor for ion channel function: how and why? *Annu Rev Biophys* 37, 175–195.
- van Eunen K, Bouwman J, Daran-Lapujade P, Postmus J, Canelas AB, Mensonides FIC, Orij R, Tuzun I, van den Brink J, Smits GJ, et al. (2010). Measuring enzyme activities under standardized in vivo-like conditions for systems biology. *FEBS J* 277, 749–760.
- Wang X, Zhang X, Dong X-P, Samie M, Li X, Cheng X, Goschka A, Shen D, Zhou Y, Harlow J, et al. (2012). TPC proteins are phosphoinositide-activated sodium-selective ion channels in endosomes and lysosomes. *Cell* 151, 372–383.
- Yamamoto A, DeWald DB, Boronenkov IV, Anderson RA, Emr SD, Koshland D (1995). Novel PI(4)P 5-kinase homologue, Fab1p, essential for normal vacuole function and morphology in yeast. *Mol Biol Cell* 6, 525–539.
- Yenush L, Mulet JM, Ariño J, Serrano R (2002). The PPZ protein phosphatases are key regulators of K⁺ and pH homeostasis: implications for salt tolerance, cell wall integrity and cell cycle progression. *EMBO J* 21, 920–929.
- Zhou X, Su Z, Anishkin A, Haynes WJ, Friske EM, Loukin SH, Kung C, Saimi Y (2007). Yeast screens show aromatic residues at the end of the sixth helix anchor transient receptor potential channel gate. *Proc Natl Acad Sci USA* 104, 15555–15559.
- Zieger M, Mayer A (2012). Yeast vacuoles fragment in an asymmetrical two-phase process with distinct protein requirements. *Mol Biol Cell* 23, 3438–3449.